

Dye-sensitized Solar Cells Based on TiO₂ Nanotube/Nanoparticle Composite as Photoanode and Cu₂SnSe₃ as Counter Electrode

C.B. Song, Y.L. Zhao^{*}, D.M. Song, L. Zhu, X.Q. Gu, Y.H. Qiang

School of Materials Science and Engineering, China University of Mining and Technology, Xuzhou 221116, China

*E-mail: sdyulong@cumt.edu.cn

Received: 20 January 2014 / Accepted: 7 February 2014 / Published: 23 March 2014

Dye-sensitized solar cells (DSSCs) based on TiO₂ nanotube/nanoparticle (NT/NP) photoanodes and Cu₂SnSe₃ (CTSe) counter electrodes were fabricated. The effect of the thickness of the CTSe films on the DSSC performance was investigated. It was found that DSSC efficiencies firstly increased and then decreased with increasing the film thickness. The optimized DSSC efficiency of 3.14% was achieved at a suitable film thickness (2.9 μm). This work presents a new approach for developing low-cost alternative for expensive Pt in TiO₂-nanotube-based DSSCs.

Keywords: dye-sensitized solar cells; Cu₂SnSe₃; TiO₂ nanotubes; photoanodes; counter electrodes

1. INTRODUCTION

Dye-sensitized solar cells (DSSCs) have attracted considerable attention as a potential alternative to the silicon related solar cells owing to both the high efficiency and low cost since 1991 [1]. A typical DSSC device consists of a dye-sensitized TiO₂ photoanode, a liquid electrolyte and a Pt-coated counter electrode [2]. Up to now, optimized DSSC in the liquid electrolyte structure has reached a considerable efficiency of 12.3% [3], which is still low compared to the 13-25% efficiency observed for Si photovoltaic cells.

An important step in the fabrication of DSSCs is to seek for photoanodes that enhance the electron transport and reduce the interfacial charge recombination [4]. In recent years, one-dimensional (1D) nanostructures such as TiO₂ NT arrays have received particular attention due to a direct and fast transport passway for carriers [5, 6]. Compared to the hydrothermal or template approaches, anodic oxidation is more convenient and simpler to obtain uniform and orderly arranged TiO₂ NTs [7]. By

varying the fluorides and changing the aqueous electrolytes, high aspect ratio and smooth surface TiO_2 NT arrays could be fabricated [8, 9]. Although the investigation of TiO_2 NT arrays applied in DSSCs was carried out and showed exciting results, a free-standing TiO_2 NT array may have wider application and better performance than the NT membrane on a Ti substrate [10, 11].

Counter electrode (CE) is an important component in the DSSC, which collects electrons from external circuit and catalyzes the reduction of triiodide ions in electrolyte [12]. As a conventional CE, Pt is scarce and expensive that makes the cost of DSSCs high and limits the potential large-scale application [13-15]. Therefore, efforts have been made on the preparation of inorganic compounds as substitute of Pt CE due to their unique characteristics such as broad variety of materials, good plasticity and simple preparation [16, 17]. As far as we know, the films of $\text{Cu}_2\text{ZnSnS}_4$ (CZTS) have been demonstrated as an effective CE material in low-cost DSSCs [18]. Wu and his coworkers shown that $\text{Cu}_2\text{ZnSnSe}_4$ (CZTSe) had a high electrocatalytic activity, leading to a DSSC efficiency of 3.85%. [19]. Similar with CZTS or CZTSe, Cu_2SnSe_3 (CTSe) belonging to the family of chalcogenide is expected to provide excellent electrocatalytic properties. However, there are still few reports on the application of CTSe in DSSCs up to now.

In order to seek a low cost candidate for Pt CE in TiO_2 -nanotube-based DSSCs, in this study, we first succeeded in assembly of DSSCs based on TiO_2 NT/NP composite photoanodes and CTSe CEs. Meanwhile, the effect of the thickness of CTSe films on the total performance of DSSCs was investigated.

2. EXPERIMENTAL

2.1 Synthesis of CTSe NPs and preparation of CEs

CTSe NPs were synthesized by a solvothermal approach. Copper (II) sulfate (1 mmol), Stannic chloride hydrated (0.5 mmol) and Se (1.5 mmol) were dissolved in distilled water (20 mL) under stirring, then ethylenediamine monohydrate (40 mL, 98%) was added. After being maintained in autoclave at 200 °C for 24 h, the precipitates were centrifuged and washed several times with distilled water and absolute ethanol. All reagents were purchased from Aladdin without any further purification. After being vacuum-dried at 60 °C for 12 h, the final dark product was dissolved in isopropanol concentrated to 150 $\text{mg}\cdot\text{mol}^{-1}$ and ultrasonicated for 10 min to form uniform “ink”. The “ink” with volume of 0.1, 0.2, 0.3 and 0.4 mL was then drop-casted onto the cleaned FTO substrate (15 Ω/\square , Dalian Hepta Chroma). The drop-casted area was controlled to be $1\times 1\text{ cm}^2$. The films were vacuum-dried fully at room temperature for 24 h and subsequently annealed at 500 °C for 35 min in selenium vapor to obtain CTSe thin films as CEs.

2.2 Preparation of free-standing NT arrays and photoanodes

TiO_2 NT arrays were formed by an optimized three-step anodic oxidation, according to our previous research paper [20]. Typically, a Ti foil was dipped into a solution of ethylene glycol

containing 0.3 wt% ammonium fluoride (NH_4F) and 2 vol% H_2O while a voltage of 60 V was applied with a Pt counter electrode for 1 h, 3 h and 1 h, respectively. After anodization, the membrane was ultrasonically washed, followed by annealing at 450 °C for 1 h. Finally, the sample was immersed in 10% H_2O_2 aqueous solution in order to detach TiO_2 NT arrays membrane from Ti substrate. TiO_2 NPs pastes (size about 10 nm, Wuhan Geao.) were printed on the FTO glass substrates by spin-coating. The trimmed TiO_2 NT array membranes ($5 \times 5 \text{ mm}^2$) were then transferred onto the TiO_2 NPs layers and the samples were annealed at 450 °C for 1 h. The above prepared samples were immersed into a 3 mM ethanol solution of N719 (Dalian Hepta Chroma) for 24 h as photoanodes.

2.3 Assembly of DSSCs

The solar cells were assembled in a typical sandwich-type cell by placing the dye-absorbed photoanodes on the CTSe-coated and Pt-coated CEs as shown in Fig. 1. The photoanodes were separated from CEs by applying a 60 μm thick thermal-plastic surlyn (DHS-SN1760) as the spacer then the assembled DSSCs were clipped together and heated to 100 °C for 10 min for encapsulation. Iodide-based liquid electrolyte (0.6 M DMPII, 0.03M I_2 , 0.5 M TBP and 0.1 M LiI in MPN, Dalian Hepta Chroma) was injected into the devices by capillary force.

2.4 Characterization and measurements

The morphology, structure and composition were characterized by X-ray diffraction (XRD, D8 Advance), energy dispersive spectrometer (EDS, Hitachi S-4800), field-emission scanning electron microscopy (FESEM, S-4800) and transmission electron microscopy (TEM, Jeol-2010). Photocurrent density-voltage (J - V) characteristics were recorded with a Keithley model 2420 digital source meter under illumination of $100 \text{ mW} \cdot \text{cm}^{-2}$ provided by a solar simulator (Newport Oriel Sol3A, 94023).

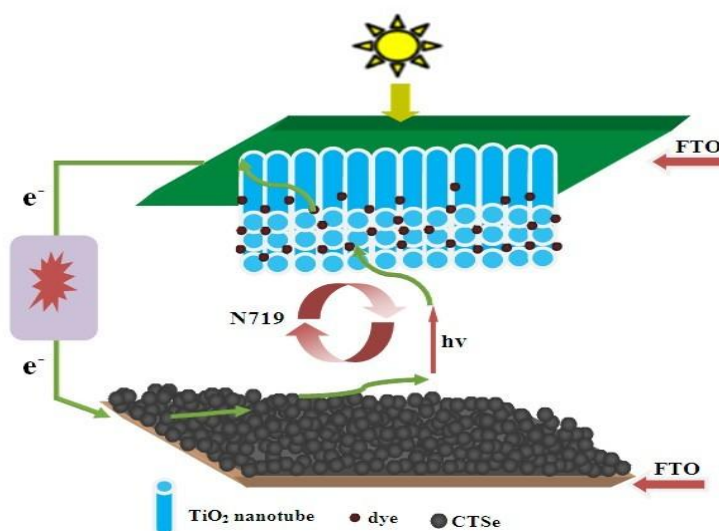


Figure 1. Scheme for DSSCs based on NT/NP photoanodes and CTSe CEs.

3. RESULTS AND DISCUSSION

Fig. 2a presents the XRD pattern of the annealed CTSe nanocrystals. All the peaks can be well indexed to standard cubic structure CTSe (JCPDS #65-4145), implying that the CTSe NPs are crystallized well after annealing. Further, the EDS spectrum confirms that the sample is exactly composed of Cu, Sn and Se elements (Fig. 2b). Taking the Sn element as the reference, the atom ratio of Cu, Sn and Se is determined to be 1.92:1.06:3.04. Considering the error of the EDS detector (approximately ± 2 atomic %), the value is almost stoichiometric. Fig. 2c shows a typical XRD pattern of the TiO₂ NT arrays. It is seen that most of the diffraction peaks except the information from Ti substrate can be assigned to the crystal planes from standard TiO₂ anatase phase (JCPDS #21-1272), suggesting that the arrays are crystallized well after annealing. On the basis of the above analysis, we can conclude that the CTSe and TiO₂ samples are single phase and nearly stoichiometric.

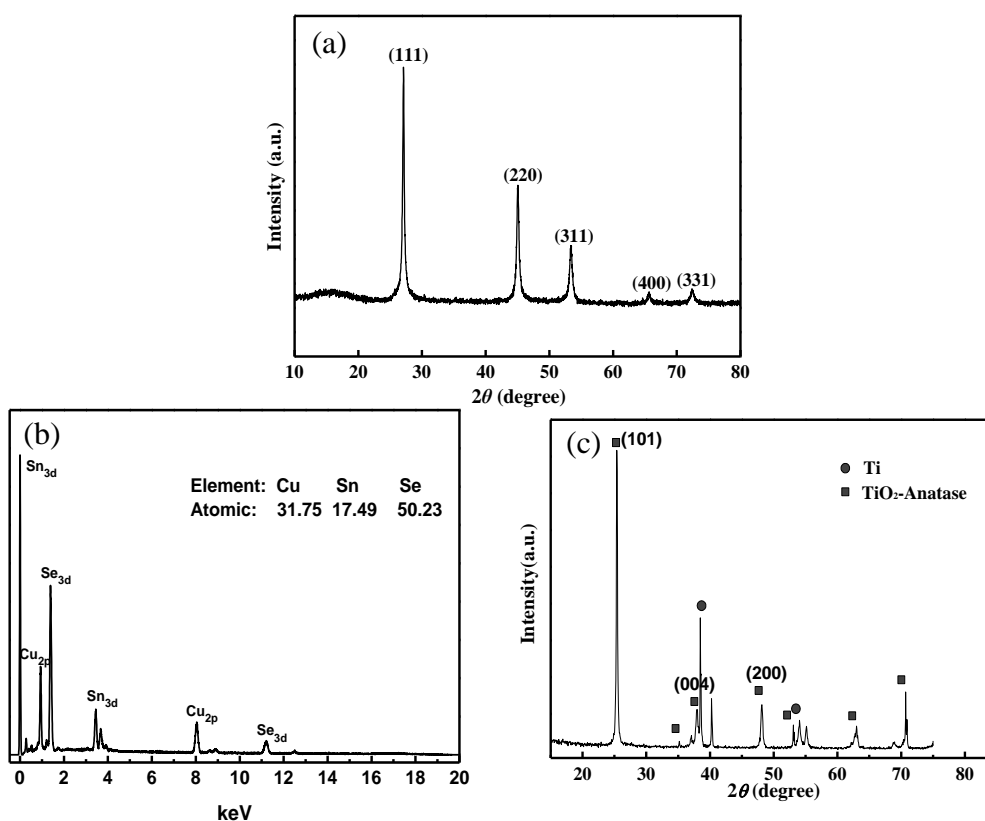


Figure 2. (a) XRD pattern and (b) EDS spectrum of CTSe NPs after annealing. (c) XRD pattern of TiO₂ NT arrays on the Ti substrate after annealing.

The morphology of as-synthesized CTSe NPs is demonstrated by FESEM and TEM images. As shown in Fig. 3a, the as-synthesized CTSe NPs are relatively uniform spheres with the diameter ranging 20-30 nm. Fig. 3b displays the TEM images of CTSe NPs, the diameters of the NPs are in accordance with the FESEM results. Fig. 3c and d display both the macroscopic and microscopic views of the surface morphologies of a TiO₂ NT array membrane which is detached from the

underlying Ti substrate. It is found that the membrane is composed of many uniform, aligned, and densely packed TiO₂ NTs with the diameters of ~100 nm, and no micro-cracks are observed.

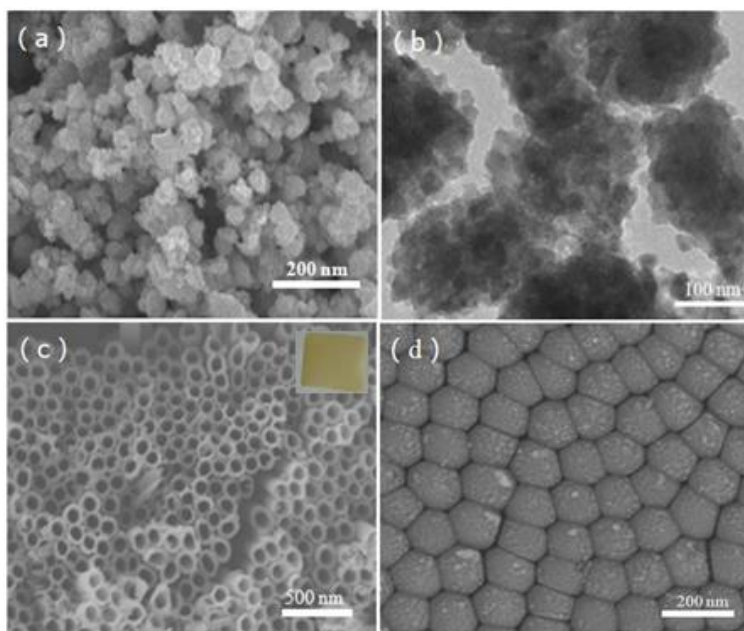


Figure 3. (a) FESEM image and (b) TEM image of CTSe nanoparticles. (c) Top view of the TiO₂ NT array, the inset is a digital photograph of the free-standing TiO₂ NT array membrane. (d) Bottom view of the TiO₂ NT array.

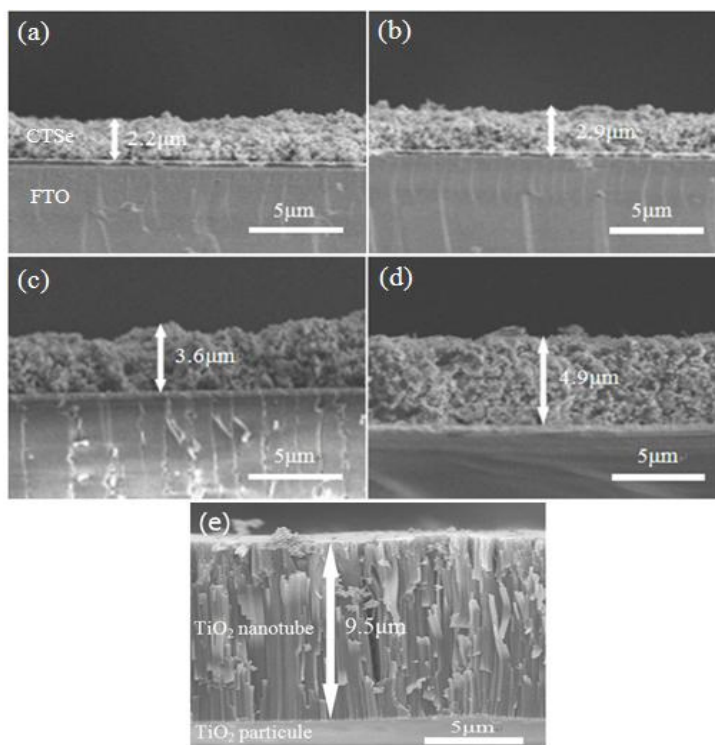


Figure 4. Cross-sectional FESEM images of CTSe thin film with volume of (a) 0.1, (b) 0.2, (c) 0.3 and (d) 0.4 mL. (e) Side view of the TiO₂ NT/NP electrode.

Fig. 4a-d displays the cross-sectional FESEM images of the CTSe thin films after annealing. Increasing the drop volume gives rise to an increase in film thickness, from 2.2 to 4.9 μm . Fig. 4e shows the side-view image of the TiO_2 NT/NP electrode. A clear, abrupt interface is observed between the layers, suggesting that an expected bilayer structure is obtained. As also can be seen, the TiO_2 NTs are perpendicular to the substrate with the thickness of $\sim 9.5 \mu\text{m}$.

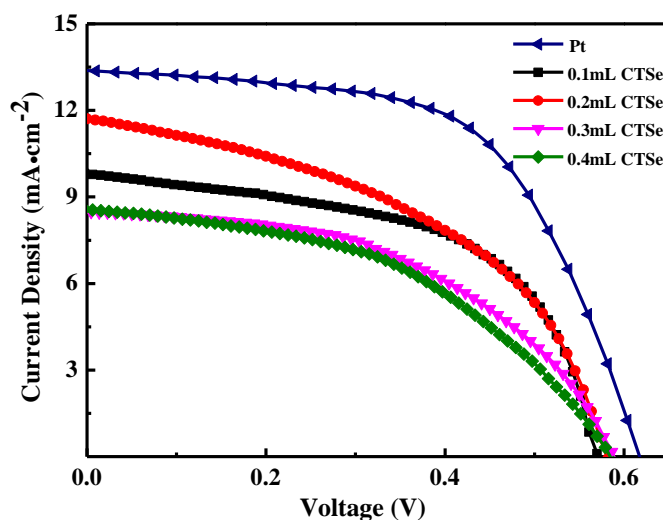


Figure 5. J - V curves of the DSSCs based on TiO_2 NT/NP photoanodes and different CEs.

Table 1. Photovoltaic parameters of DSSCs based on TiO_2 NT/NP photoanodes and different CEs.

Drop volume mL	Thickness μm	J_{sc} $\text{mA}\cdot\text{cm}^{-2}$	V_{oc} V	FF %	η %
0.1	2.2	9.78	0.570	55.43	3.09
0.2	2.9	11.71	0.573	45.80	3.14
0.3	3.5	8.55	0.579	49.28	2.44
0.4	4.9	8.45	0.585	45.39	2.30
Pt	0.1	13.4	0.626	58.21	4.90

Fig. 5 displays the J - V curves of DSSCs based on TiO_2 NT/NP photoanodes and CTSe CEs with different thickness. Meanwhile, the corresponding photovoltaic parameters are summarized in Table 1, including short-current density (J_{sc}), open-circuit voltage (V_{oc}), fill factor (FF) and photoelectric conversion efficiency (η). As seen, the η of DSSCs firstly increases and then decreases with increasing the thickness of CTSe films. At an optimum thickness of 2.9 μm , the η reaches the highest value of 3.14%. Naturally, the enhanced DSSC performance is mainly associated with a remarkable increase in J_{sc} . The prepared CTSe film is composed of nanoparticles and porous (Fig. 4). With the increase in the film thickness, CTSe CE provides relatively larger amount of electrocatalytic sites that is beneficial to the electrocatalytic activity and leads to the increase of J_{sc} [21]. On the other

hand, it can be seen clearly that the η decreases significantly with further increasing the film thickness (3.6 μm and 4.9 μm), which is caused by the decrease of J_{sc} . The decline of J_{sc} may be attributed to high resistance for charge transport, caused by more abundant grain boundaries and defects in thicker film [22]. In a word, this behavior might be presumably attributed to a competition from the enhanced electrocatalytic activity and the decreased charge transport. Compared with the Pt CE, though the photovoltaic properties of CTSe CEs are lower, the CTSe CEs are confirmed to have good electrocatalytic activity. Further improvement of the photovoltaic performance is expected, as many parameters of the CE preparation, such as the film density, assembly technology of solar cells, and so on.

4. CONCLUSIONS

In summary, CTSe NPs were synthesized by a facile solvothermal method and free-standing TiO₂ NT arrays were prepared by a three-step anodization. Moreover, DSSCs based on TiO₂ NT/NP photoanodes and CTSe CEs have been fabricated. Photovoltaic measurement showed that the power conversion efficiency of DSSCs firstly increased and then decreased with increasing the thickness of CTSe films. Therefore, an optimum thickness of 2.9 μm associated with the maximum conversion efficiency of 3.14% was achieved. CTSe CE can be used in TiO₂-nanotube-based DSSCs and has good electrocatalytic activity, which has a promising application prospect.

ACKNOWLEDGEMENTS

This work was financially supported by the Fundamental Research Funds for the Central Universities (2013XK07) and Natural Science Foundation of Jiangsu Province (BK20130198).

References

1. B. O'Regan, M. Grätzel, *Nature*, 353 (1991) 737
2. J. Sheng, L.H. Hu, S.Y. Xu, W.Q. Liu, L. Mo, H.J. Tian, S.Y. Dai, *J. Mater. Chem.*, 21 (2011) 5457
3. A. Yella, H.W. Lee, H.N. Tsao, C. Yi, A.K. Chandiran, M.K. Nazeeruddin, E.W.G. Diau, C.Y. Yeh, S.M. Zakeeruddin, M. Grätzel, *Science*, 334 (2011) 629
4. V. Mani, S.M. Chen, B.S. Lou, *Int. J. Electrochem. Sci.*, 8 (2013) 11641
5. K. Zhu, N.R. Neale, A. Miedance, A.J. Frank, *Nano Lett.*, 7 (2007) 69
6. O.K. Varghese, M. Paulose, C.A. Grimes, *Nature Nanotech.*, 4 (2009) 592
7. J.P. Yan, F. Zhou, *J. Mater. Chem.*, 21 (2011) 9406
8. J.M. Macak, H. Tsuchiya, L. Taveira, S. Aldabergerova, P. Schmuki, *Angew. Chem. Inter. Edit.*, 44 (2005) 7463
9. Q.Y. Cai, M. Paulose, O.K. Varghese, C.A. Grimes, *J. Mater. Res.*, 20 (2005) 230
10. Q.W. Chen, D.S. Xu, *J. Phys. Chem. C*, 113 (2009) 6310
11. X.F. Gao, J.H. Chen, C. Yuan, *J. Power Sources*, 240 (2013) 503
12. S.J. Peng, J. Liang, S.G. Mhaisalkar, S. Ramakrishna, *J. Mater. Chem.*, 22 (2012) 5308
13. A. Kay, M. Grätzel, *Sol. Energy Mater. Sol. Cells*, 44 (1996) 99
14. B. O'Regan, D.T. Schwartz, S.M. Zakeeruddin, M. Grätzel, *Adv. Mater.*, 12 (2000) 1263

15. J. E. Trancik, S.C. Barton, J. Hone, *Nano Lett.*, 8 (2008) 982
16. G.R. Li, J. Song, G.L. Pan, X.P. Gao, *Energy Environ. Sci.*, 4 (2011) 168
17. K. Miettunen, M. Toivola, G. Hashmi, J. Salpakari, I. Asghar, P. Lund, *CARBON*, 49 (2011) 528
18. X. Xin, M. He, W. Han, J. Jung, Z. Lin, *Angew. Chem. Inter. Edit.*, 50 (2011) 11739
19. Y.F. Du, J.Q. Fan, W.H. Zhou, Z.J. Zhou, J. Jiao, S.X. Wu, *ACS Appl. Mater. Interfaces*, 4 (2012) 1796
20. D. M. Song, Y.H. Qiang, Y.L. Zhao, X.Q. Gu, C.B. Song, *Appl. Surf. Sci.*, 277 (2013) 53
21. M.X. Wu, X. Lin, A. Hagfeldt, T.L. Ma, *Angew. Chem. Inter. Edit.*, 4 (2011) 1680
22. G.R. Li, F. Wang, Q.W. Jiang, X.P. Gao, P.W. Shen, *Angew. Chem. Inter. Edit.*, 122 (2010) 3735

© 2014 The Authors. Published by ESG (www.electrochemsci.org). This article is an open access article distributed under the terms and conditions of the Creative Commons Attribution license (<http://creativecommons.org/licenses/by/4.0/>).